A finger-jointing model for describing nanostructures of cellulose microfibrils

Bunshi Fugetsu (bunshifugetsu@g.ecc.u-tokyo.ac.jp)
University of Tokyo
Adavan Kiliyankil Vipin
University of Tokyo
Shoichi Takiguchi
University of Tokyo
Ichiro Sakata
University of Tokyo
Morinobu Endo
Shinshu University

Research Article

Keywords: TEMPO, CNFs, spectroscopy, working and resting rhythm

Posted Date: January 15th, 2021

DOI: https://doi.org/10.21203/rs.3.rs-145491/v1

Abstract

We propose a finger-jointing model to describe the possible nanostructures of native cellulose microfibrils based on new observations obtained through thermal decomposition of 2,2,6,6-tetramethylpiperidine-1-oxyl (TEMPO) oxidized cellulose nanofibers (CNFs) in saturated water vapor. We heated the micrometers-long TEMPO-CNFs in saturated water vapor (≥ 120 °C, ≥ 0.2 MPa) for ≤ 8 h. The long TEMPO-CNFs unzipped into short (100 s of nanometers long) cellulose nanowhiskers (CNWs). We characterized the CNWs using Raman spectroscopy and Fourier transform infrared spectroscopy, observing similar spectra as TEMPO-CNFs. Thus, the native cellulose microfibrils are not seamlessly long structures, but serial "jointed structures" of CNWs. The finger-jointing model implies a "working and resting rhythm" in the biosynthesis of cellulose. CNWs are highly dispersible in water and polar organic solvents, and are much easier to combine with other classes of polymers at nano-levels. The findings can enhance the feasibility and applicability of native cellulose to achieve sustainable development goals.

Background

Plant cellulose is the most abundant biomass on Earth. Native plant cellulose appears as fibers approximately 1-3 mm in length and 30 μm in width. The macro-sized plant cellulose exhibits drastic changes in both its physiochemical and mechanical properties when split down to nano-size. Nano-sized cellulose, or nanocellulose, is classified further as cellulose nanofibers (CNFs) and cellulose nanocrystals (CNCs). Use of 2,2,6,6-tetramethylpiperidine-1-1oxyl (TEMPO)[1] as a catalyst to regioselectively oxidize C6 primary hydroxyls to C6 carboxylates in aqueous media is a standard procedure, among other methodologies,[2-5] for splitting the macro-sized plant cellulose down to CNFs. TEMPO oxidized CNFs (TEMPO-CNFs) are truly fiber-shaped with a nearly uniform width of approximately 3 nm and a length of a few micrometers.[6] Thin films made up entirely of TEMPO-CNFs are highly transparent and have excellent tensile strength (200 ~ 300 MPa),[6] excellent elastic moduli (6 ~ 7 GPa), and excellent thermal expansion coefficiencies (2.7 ppm K^{-1}).[7] The presence of abundant carboxylates on the surface is another advantage of TEMPO-CNFs. Counterions of the carboxylates are commonly sodium ions, but they can be either partly or completely replaced (exchanged) with any kind of cations. When coupled with copper (II) ions as their counterions, TEMPO-CNFs are capable of eliminating ammonia, trimethylamine, hydrogen sulfide, and methyl mercaptan from the air.[8] As templates, TEMPO-CNFs are useful for synthesizing water-insoluble Prussian blue nanoparticles for selective elimination of radioactive cesium ions.[9, 10] As additives, both the tensile strength and elastic moduli of organic polymers, such as hydrogenated nitrile-butadiene rubbers,[11] are remarkably improved by adding a certain amount of TEMPO-CNFs to the matrix; however, the uniform dispersion of TEMPO-CNFs in the matrix still remains a challenge. TEMPO-CNFs have recently been produced in industrial quantities, and their potential applications have been explored worldwide.[12, 13]

In contrast, CNCs are spindle-shaped with lengths ≤ 200 nm and widths of 5 - 20 nm. Hydrolysis of native plant cellulose in acidic media under mild heat (e.g., 64% H_2SO_4 at 70°C) is the basic method[14] used for

preparing CNCs. Other oxidants, such as periodate[15] and chlorite,[16] are also applicable for preparing CNCs. CNCs also contain some negatively charged moieties, as do TEMPO-CNFs. The degree of crystallinity for CNCs is commonly higher than that of TEMPO-CNFs. CNCs have recently been produced in industrial quantities, and a wide range of materials, from organic polymers to inorganic nanoparticles, can be combined with CNCs to improve their physiochemical and/or mechanical properties. [17,18]

Results And Discussions

Unlike CNFs and CNCs in both morphology and physiochemical properties, we produced a new class of nanocellulose by thermally decomposing TEMPO-CNFs in saturated water vapor. We experimentally demonstrate that shorter, thinner, whisker-shaped nanocellulose can be produced in one step via thermal decomposition.

We thermally decomposed an aqueous suspension containing 0.2 wt% TEMPO-CNFs at 150 °C for 4 h. Figure 1a shows AMF images of the shorter, thinner, whisker-shaped nanocellulose that resulted, which we specified as “cellulose nanowhiskers” (CNWs). Thirty CNWs were randomly selected and the length and width measured. The CNWs had lengths of 400–600 nm and widths of 1.5-3.0 nm.

The temperature of the saturated water vapor and the thermal decomposition time are the two key parameters affecting the morphology of TEMPO-CNFs. Under low temperature and short time, TEMPO-CNFs remained almost unchanged. However, under higher temperatures and longer thermal reaction times, TEMPO-CNFs changed partly or completely into CNWs. Figure 1b and Fig. 1c show typical AFM images of the same sample as in Fig. 1a but thermally treated at 150 °C for 2 hours. We observed CNWs and CNFs with shorter lengths (0.8–1.5 μm). Under soft thermal reaction conditions (e.g., 120 °C/6 h, 130 °C/4 h, 140 °C/2 h, and 150 °C/1.5 h), the thermally treated aqueous TEMPO-CNF suspensions are nearly colorless or lightly yellowish and highly transparent. Under mild thermal reaction conditions (e.g., 150 °C/4 h, 160 °C/3 h, and 180 °C/2 h), the thermally treated aqueous TEMPO-CNF suspensions are a heavy brown color and become hydrogels under tougher thermal reaction conditions (e.g., 150 °C/6 h, 160 °C/5 h, and 180 °C/4 h). A photo of four thermally treated aqueous TEMPO-CNF suspensions is given in the supporting information (Figure S1); TEMPO-CNFs were thermally treated for 2 h, 3 h, 4.5 h, and 5 h at 140 °C in the saturated water vapor.

Water is vaporized from the thermally treated aqueous suspension in an electrical heating oven at a constant temperature of 40 °C and obtained a yellowish film. The yellowish substance is transferred to the solution after washing the film 3–5 times with an aqueous solution containing 70% ethanol (Figure S2). The colorless, transparent film of CNWs is used to measure their physiochemical properties by Raman and Fourier transform infrared spectroscopy (FT-IR). The aqueous sample was prepared by thermal decomposition of the aqueous suspension containing 0.2 wt% TEMPO-CNFs at 150 °C for 4 h in the saturated water vapor.

Figure 2 shows the typical Raman spectra. Raman peaks corresponding to the skeletal vibrational modes of the asymmetric vibration of C-O-C at 1098 cm^{-1} (ν_{as}) and the symmetric vibration of C-O-C at 1120 cm^{-1} (ν_{s}) of the β (1–4) glycosidic linkage of the β-D-glucopyranosyl units[19 – 23] of cellulose were clearly observed. A Raman peak corresponding to the stretching model of breathing vibrations of the glucopyranose rings (-C-C-) at 1153 cm^{-1} [19 – 23] was also observed. Raman peaks were also observed in the 1300–1500 cm^{-1} frequency region provide insights into the crystallinity and length/thickness of the multiple packed polysaccharide chains. The Raman spectra of TEMPO-CNFs are also given in Fig. 2 for comparisons.

The CNW-based films were also characterized by FT-IR. Four samples prepared by thermal decomposition of an aqueous solution containing 0.2 wt% TEMPO-CNFs at 135 °C, 140 °C, 150 °C, and 160 °C for 2 h. Spectra identical to that of cellulose were observed.[24 – 27] Fig. 3 shows the following spectra: 1100 – 900 cm^{-1}, C-O-C stretching; 3600 – 3200 cm^{-1}, O-H stretching; and the distinguishing peak of COO^{-} at 1600 cm^{-1}. Notably, under tougher thermal reaction conditions (e.g., 160 °C/2 h), the intensity of the carboxylate peak (1600 cm^{-1}) decreased sharply, indicating that the carboxylated polysaccharide chains situated on the outmost layers of the TEMPO-CNFs had detached. The uncharged nanocellulose exhibited a tendency to form hydrogels due to the external hydrogen bonding interactions.

Both the Raman and FT-IR spectra suggest physicochemically that CNWs are built up by multiple packed cellulose (polysaccharide) chains. TEMPO-CNFs changed drastically from longer nanofibers to shorter nanowhiskers in saturated water vapor under vapor pressures ≥ 0.2 MPs and temperature ≥ 120 °C. The drastic change in the lengths of TEMPO-CNFs gave new insights into the nanostructures of cellulose microfibrils. From our experimental observations, it is reasonable to assume that the native cellulose microfibrils are not seamlessly long nanofibers, but are “jointed structures”.

We propose a new model, as shown in Fig. 4, to describe the possible nanostructures of the native cellulose microfibrils. Key concepts of this newly proposed model are summarized as follows:

i. The native cellulose microfibrils are not seamlessly long structures, but are combined and jointed structures composed of many shorter blocks that are jointed in a simple jointing manner;
ii. Finger-jointing is the simple manner by which the shorter blocks were jointed in to longer lengths of cellulose microfibrils;
iii. Finger-jointing structures enable cellulose microfibrils to twist, [28] to curve, and to transform from crystalline structures to amorphous structures;
iv. Finger-jointing structures are much weaker than the multiple-chain packed structures (24–36 of the polysaccharide chains have packed together in a single microfibril[28, 29]). In other words, the finger-jointing structures have largely or completely been destroyed under saturated water vapor, but the multiple-chain packed basic structures remain unchanged;
v. From the biosynthesis point of view, plants are not working all day for biosynthesis of cellulose, but working and resting rhythms may also exist in the plant world;

vi. Cellulose synthase is found along the edges of each polysaccharide chain so that the newly synthesized polysaccharide chains can be naturally jointed;

vii. After the microfibrils have been unzipped down to CNWs, the polysaccharide chains situated on the outmost layer are in the weakest situations are detached from the main body of the CNWs under tougher thermal reaction conditions.

CNWs are highly dispersible in both water and polar organic solvent, such as dimethyl sulfoxide (DMSO), n-methylpyrrolidone (nMP), N,N-dimethylformamide (DMF), and alcohols. In contrast, TEMPO-CNFs are extremely difficult to disperse in water, DMSO, nMP, DMF, and alcohols due to their high tendency to form aggregates. At identical concentrations (i.e., 0.2 wt% in water), CNWs had a viscosity as low as water, whereas TEMPO-CNFs had a viscosity approximately 5–8 times higher than that of CNWs.

As additives, CNWs can easily be combined with other kinds of polymers at nano-levels of combinations. For example, CNWs combined with polytetrafluoroethylene (PTFE) nanoparticles via solution/emulsion affords PTFE/CNW hybridized films. The PTFE/CNW hybridized film contained only 0.6% CNWs but behaved like a piece of paper, capable of absorbing water and turning from translucent to transparent (Fig. 5).

Conclusions

Plant cellulose can be key to achieving the goals of SDGs. Nevertheless, the basic polysaccharide blocks, the cellulose microfibrils, are the “god-made” nanostructures, and how their structure relates to their function remains largely unknown. We have much to learn about the length of each polysaccharide chain, the degree of orientation, and the intensity of interactions among the packed polysaccharide chains. In a previous study, Li and Renneckar[30] showed that TEMPO-CNFs can be split down to a single or double digit Angstrom thickness with 100 s of nanometers in length under extensive ultra-sonication. This experimental observation also suggests that cellulose microfibrils are not seamlessly ultra-long, structured substances. In other words, plants are not working all day to synthesize cellulose, but a working and resting rhythm exists in plants, resulting in jointed bio-products. Other “god-made” nanostructures, such as DNA and proteins, may also be a category of jointed structures and could be unzipped into basic (building) blocks once the hydrogen binding interactions among the basic blocks are weakened and/or destroyed. In conclusion, jointing of a certain number of the building blocks is a simple yet universal manner by which the giant-sized bio-structures with specified shapes and diverse functionalities are established.

Methods

TEMPO-CNFs were purchased from Dai-ichi Kogyo Seiyaku Co. Ltd. (Kyoto, Japan); they were produced via TEMPO oxidation of plant cellulose. The as-received suspension was diluted 1/10 with deionized water. The resulting suspension contained 0.2 wt% TEMPO-CNFs and was used throughout this study. Sealed thermal decomposition vessels were obtained from San-ai Kagaku Co., Ltd. (Nagoya, Japan) and

used for thermal decomposition of TEMPO-CNFs. The thermal decomposition vessels consisted of a sealed PTFE-based inner vessel and a sealed steel-based outer cylinder. Approximately 50 mL of the aqueous suspension of 0.2 wt% TEMPO-CNFs was sealed in the PTFE vessel and the sealed vessel placed in an electric heating oven for a predetermined time at a specified temperature. After the sealed vessel was cooled to room temperature, the thermally treated aqueous suspension was removed from the vessel to prepare the film samples and to characterize their physiochemical properties. To prepare the film, approximately 15 g of the thermally treated suspension was placed in a polystyrene-based petri dish and water vaporized in an electric heating oven at a constant temperature of 40 °C, obtaining a yellowish film. The yellowish substance was removed by washing the film sample with an aqueous solution containing 70% ethanol, resulting in a transparent film. The film sample was dried at a constant temperature of 40 °C overnight and then used for characterization via Raman spectrometry and FT-IR.

We used a Raman spectrometer (Renishaw, inVia Raman) with four excitation wavelengths: 488 nm, 532 nm, 633 nm, and 785 nm. The Raman measurements were performed mainly with excitation at 532 nm (exposure time 10 s, laser power 74 mW, 6 accumulations). FT-IR spectra were obtained using A Jasco FT-IR-460 Fourier Transform Infrared Spectrometer.

The atomic force microscope (AFM) used throughout this study was a PicoScan 2500™ system purchased from Molecular Imaging Co. Ltd. (Tempe, AZ, U.S.A.). The thermally treated aqueous suspension of 0.2 wt% TEMPO-CNFs was diluted about 1/10000 with 80% ethanol. Approximately 1 µl was casted on a silicon wafer (plate) and then dried under ambient temperature before analysis.

The PTFE/CNW hybridized film samples consisted of 99.4 wt% PTFE, and 0.6 wt% CNWs were prepared via solution/emulsion combination. PTFE D-210C, a milky white aqueous dispersion containing 60 wt% PTFE particles (average size, 250 nm) stabilized with nonionic surfactants, was purchased from Daikin (Osaka, Japan). Briefly, 50 ml PTFE D-210C was mixed with 50 mL of an aqueous suspension of 0.2 wt% CNWs. This mixed emulsion/solution was continuously stirred at 80 °C until a dough-like substance was obtained. The PTFE/CNW-based dough was washed thoroughly with deionized water to remove the nonionic surfactant. The washed PTFE/CNW dough was then pressed at 50 MPa 5 ~ 8 times at 80 °C to obtain a film-like PTFE/CNW substance. The PTFE/CNW film was placed in an electric oven overnight at 80 °C to remove the residual water from the film. The PTFE/CNW-based film was further pressed at 50 MPa at 270 °C for 10 min. Cooling to room temperature obtained the PTFE/CNW hybridized film sample (thickness ≈ 80 µm).

Declarations

Authors Contributions

B.F. conceived and designed this project and performed the experiments and wrote the manuscript. V.A.K. prepared the CNW-based film and performed the FT-IR measurements. S.T. performed the AMF measurements. I.S. and M.E. conceived and supervised this project.

Declaration of Competing Interest

The authors have no conflicts of interest to disclose.

Acknowledgments

This study was supported in part by grants from the project Advanced integration research for agriculture and interdisciplinary fields of the NARO Bio-oriented Technology Research Advancement Institution. The Raman measurements were conducted at the Advanced Characterization Nanotechnology Platform of the University of Tokyo, supported by the "Nanotechnology Platform" of the Ministry of Education, Culture, Sports, Science and Technology (MEXT), Japan.

References

1. Sato, Y. Nishiyama, J.-L. Putaux, M. Vignon, A. Isogai, Homogeneous suspensions of individualized microfibrils from TEMPO-catalyzed oxidation of native cellulose, Biomacromolecules 2006, 7, 1687-1691.
2. N. Nakagaito, H. Yano, The effect of morphological changes from pulp fiber towards nano-scale fibrillated cellulose on the mechanical properties of high-strength plant fiber based composite, App. Phys. A 78, 2004, 547-552.
3. Abe, S. Iwamoto, H. Yano, Obtaining cellulose nanofibers with a uniform width of 15 nm from wood, Biomacromolecules 2007, 8, 3276-3278.
4. Q. Wang, J. Y. Zhu, R. Gleisner, T. A. Kuster, U. Baxa, S. E. McNeil, Morphological development of cellulose fibrils of a bleached eucalyptus pulp by mechanical fibrillation, Cellulose 2012, 19, 1631-1643.
5. Noguchi, I. Homma, Y. Matsubara, Complete nanofibrillation of cellulose prepared by phosphorylation, Cellulose 2017, 24, 1295-1305.
6. Isogai, T. Saito, H. Fukuzumi, TEMPO-oxidized cellulose nanofibers, Nanoscale 2011, 3, 71-85.
7. Fukuzumi, T. Saito, Y. Kumamoto, T. Iwata, A. Isogai, Transparent and High Gas Barrier Films of Cellulose Nanofibers, Prepared by TEMPO-Mediated Oxidation Biomacromolecules 2009, 10, 162-165.
8. A. Kiliyankil, B. Fugetsu, I. Sakata, Z. Wang, M. Endo, Aerogels from copper (II)-cellulose nanofibers and carbon nanotubes as absorbents for the elimination of toxic gases from air, J. Colloid and Interface Sci., 582, Part B, 2020, 950-960.
9. K. Vipin, B. Fugetsu, I. Sakata, A. Isogai, M. Endo, M. Li, M. S. Dresselhaus, Cellulose nanofiber backboned Prussian blue nanoparticles as powerful adsorbents for the selective elimination of radioactive cesium, Sci. Rep. 2016, https://doi.org/10.1038/srep37009.
10. Manabe, A. K. Vipin, T. Kumashiro, S. Takiguchi, B. Fugetsu, I. Sakata, Stabilization of Prussian blue using copper sulfate for eliminating radioactive cesium from a high pH solution and seawater, J. Hazar. Mater. 2020, 386, 121979.

11. Noguchi, M. Endo, K. Niihara, H. Jinnai, A. Isogai, Cellulose nanofiber/elastomer composites with high tensile strength, modulus, toughness, and thermal stability prepared by high-shear kneading, Compos. Sci. Technol. 2020, 188, 108005.
12. Isogai, Emerging nanocellulose technologies: recent developments, Advan. Materl., DOI: 10.1002/adma.202000630.
13. Isogai, Cellulose nanofibers: recent progress and future prospects, J. Fiber Sci. Technol. 76(10), 2020, 310-326.
14. D. Edgar, D. G. Gray, Smooth model cellulose I surfaces from nanocrystal suspensions, Cellulose 2003, 10, 299-306.
15. Chen, T. G. M. van de Ven, Morphological changes of sterically stabilized nanocrystalline cellulose after periodate oxidation, Cellulose 2016, 23, 1051-1059.
16. Trilokesh, K. B. Uppuluri, Isolation and characterization of cellulose nanocrystals from jackfruit peel, Sci Rep 9, 16709 (2019). https://doi.org/10.1038/s41598-019-53412-x.
17. Habibi, L. A. Lucia, O. J. Rojas, Cellulose Nanocrystals: Chemistry, Self-Assembly, and Applications, Chem. Rev. 2010, 110, 3479-3500.
18. M. Vanderfleet, E. D. Cranston, production routes to tailor the performance of cellulose nanocrystals, Nature Reviews Materials, 2020, https://www.nature.com/articles/s41578-020-00239-y
19. G.M. Edwards, D.W. Farwell, D. Webster, FT Raman microscopy of untreated natural plant fibres, Spectrochimica Acta Part A, 1997, 53A, 2383-2392.
20. Schrader, H. H. Klump, K. Schenzel, H. Schulz, Non-destructive NIR FT Raman analysis of plants, J. Mol. Struct. 1999, 509, 201-212.
21. P. Alves, L. P.Z. de Oliveira, A. A.N. Castro, R. Neumann, L. F.C. de Oliveira, H. G.M. Edwards, A. C. Sant'Ana, The structure of different cellulose fibers characterized by Raman spectroscopy, Vibrational Spectroscopy. 2016, 86, 324-330.
22. Jahn, M.W. Schroder, M. Futing, K. Schenzel, W. Diepenbrock, Characterization of alkali treated flax fibers by means of FT Raman spectroscopy and environmental scanning electron microscopy, Spectrochimica Acta, Part A, 2002, 58, 2271-2279.
23. Gierlinger, T. Keplinger, M. Harrington, Imaging of plant cell walls by confocal Raman microscopy, Nature Protocols, 2012, 7, 1694-1708.
24. Sturcova, I. His, D.C. Apperley, J. Sugiyama, M. C. Jarvis, Structural details of crystalline cellulose from higher plants. Biomacromolecules, 2004, 5, 1333–1339.
25. Marechal, H. Chanzy, The hydrogen bond network in I-beta cellulose as observed by infrared spectrometry. J. Mol. Struct, 2000, 523, 183–196.
26. Abidi, L. Cabrales, C. H. Haigler, Changes in the cell wall and cellulose content of developing cotton fibers investigated by FTIR spectroscopy, Carbohydrate Polymers, 2014, 100, 9-16.
27. Y. Oh, D. I. Yoo, Y. Shin, G. Seo, FTIR analysis of cellulose treated with sodium hydroxide and carbon dioxide, Carbohydrate Research, 2005, 340, 417-428.

28. N. Fernandes, L. H. Thomas, C. M. Altaner, P. Callow, V. T. Forsyth, D. C. Apperley, C. J. Kennedy, M. C. Jarvis, Nanostructure of cellulose microfibrils in spruce wood, PNAS, 2011, 108 (47), E1195-E1203; https://doi.org/10.1073/pnas.1108942108.
29. Endler, S. Persson,) Cellulose synthases and synthesis in Arabidopsis. Mol Plant, 2011, 4, 199–211.
30. Li, S. Renneckar, Molecular thin nanoparticles from cellulose: isolation of sub-microfibrillar strctures, Cellulose, 2009, 16, 1025-1032.

Figures

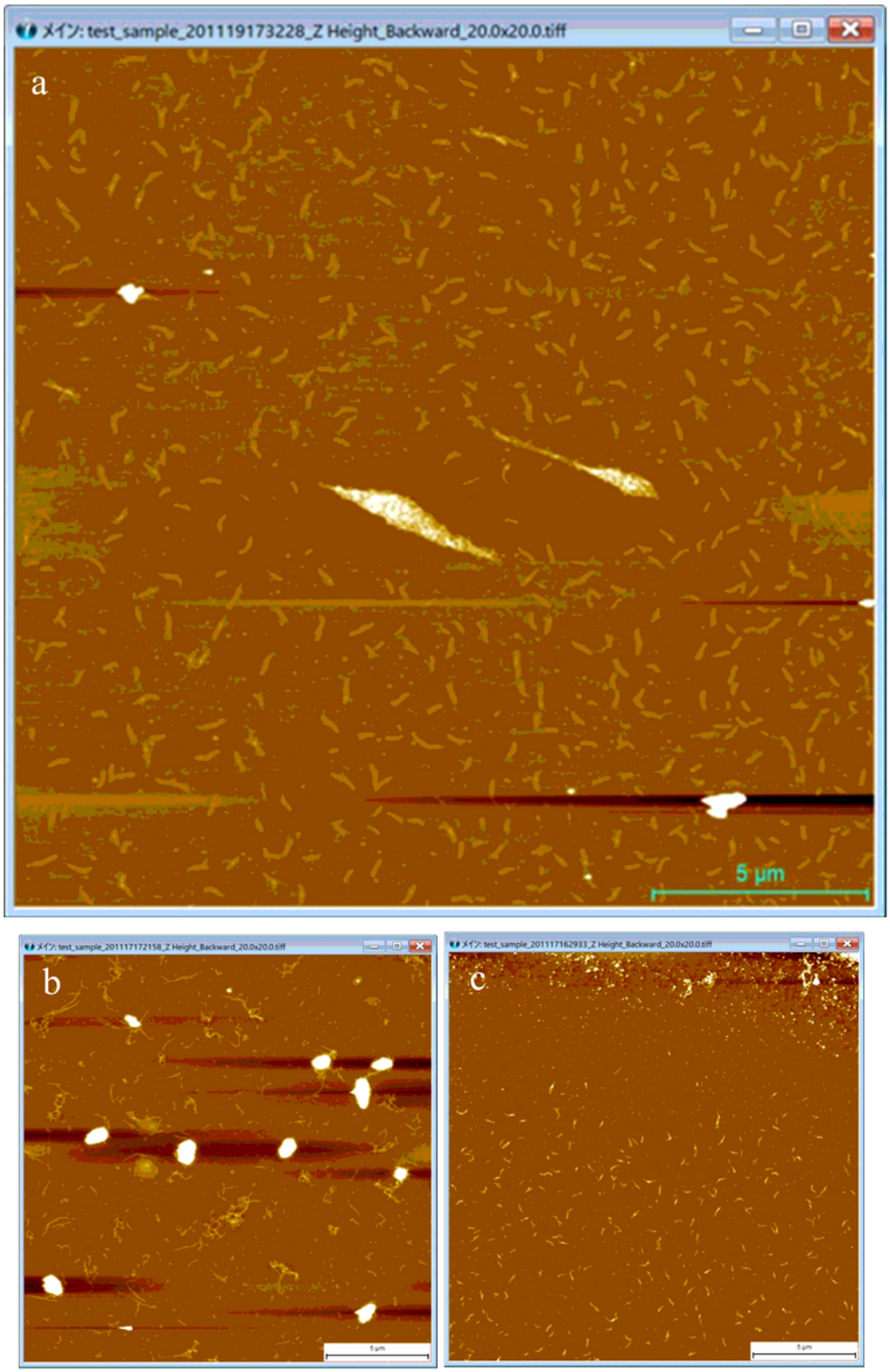

Figure 1

AFM images of cellulose nanowhiskers (CNWs) prepared by thermal decomposition of an aqueous suspension containing 0.2 wt% TEMPO-CNFs in saturated water vapor at 150°C for 2 or 4 hours. The sample was diluted 10,000 with 70% ethanol. (a) TEMPO-CNFs were unzipped into CNWs 400 – 600 nm in length and 1.5 – 3.0 nm in thickness after 4 h of decomposition. (b) After 2 h of decomposition, both CNFs with shorter lengths and (c) CNWs were observed.

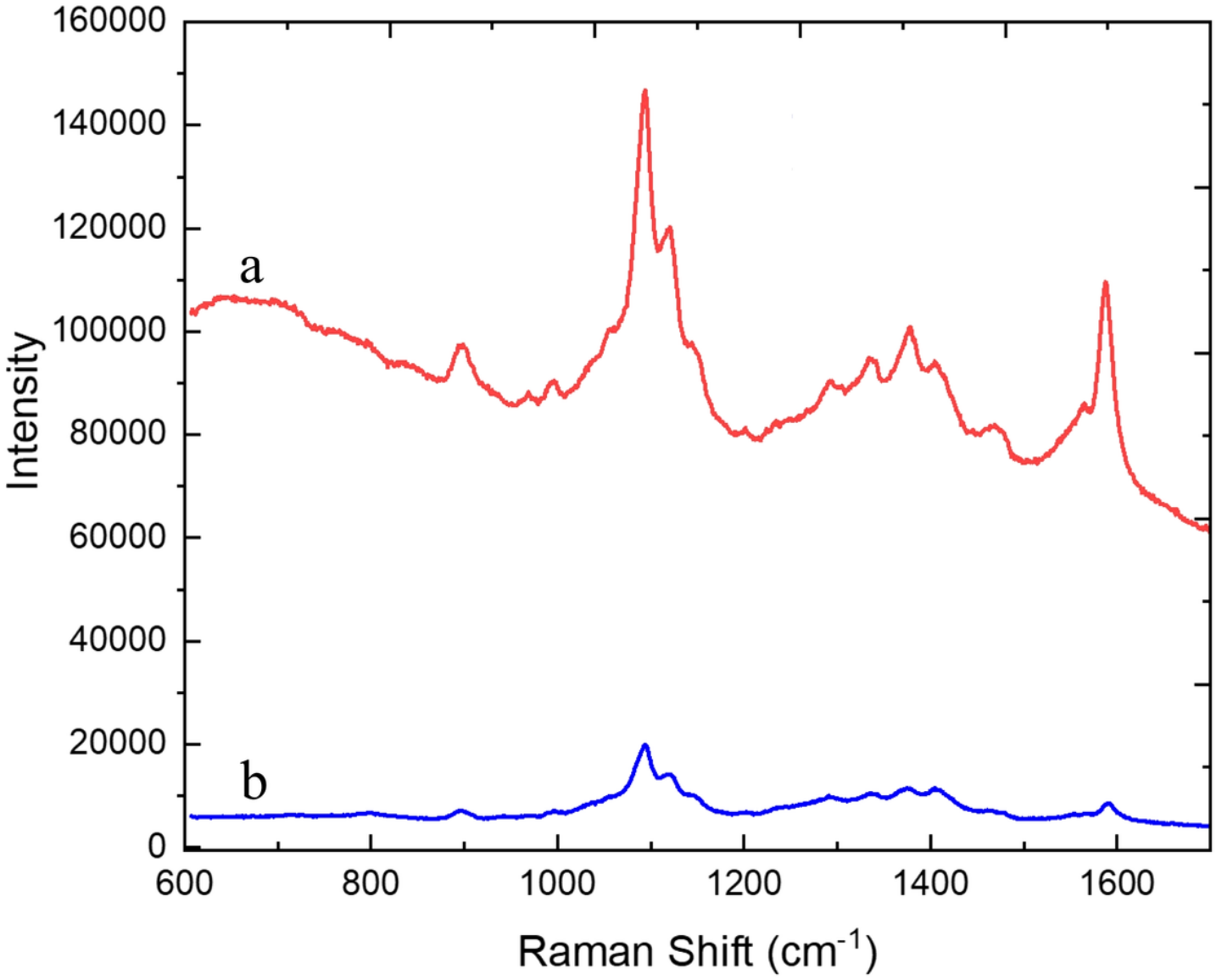

Figure 2

Raman spectra of a 5-μm-thick film sample made by using the thermally treated TEMPO-CNFs in saturated water vapor at 150°C for 4 hours (a) or the as-produced TEMPO-CNFs (b). The excitation wavelength was 532 nm, exposure time 10 s, and laser power 74 mW with 6 accumulations.

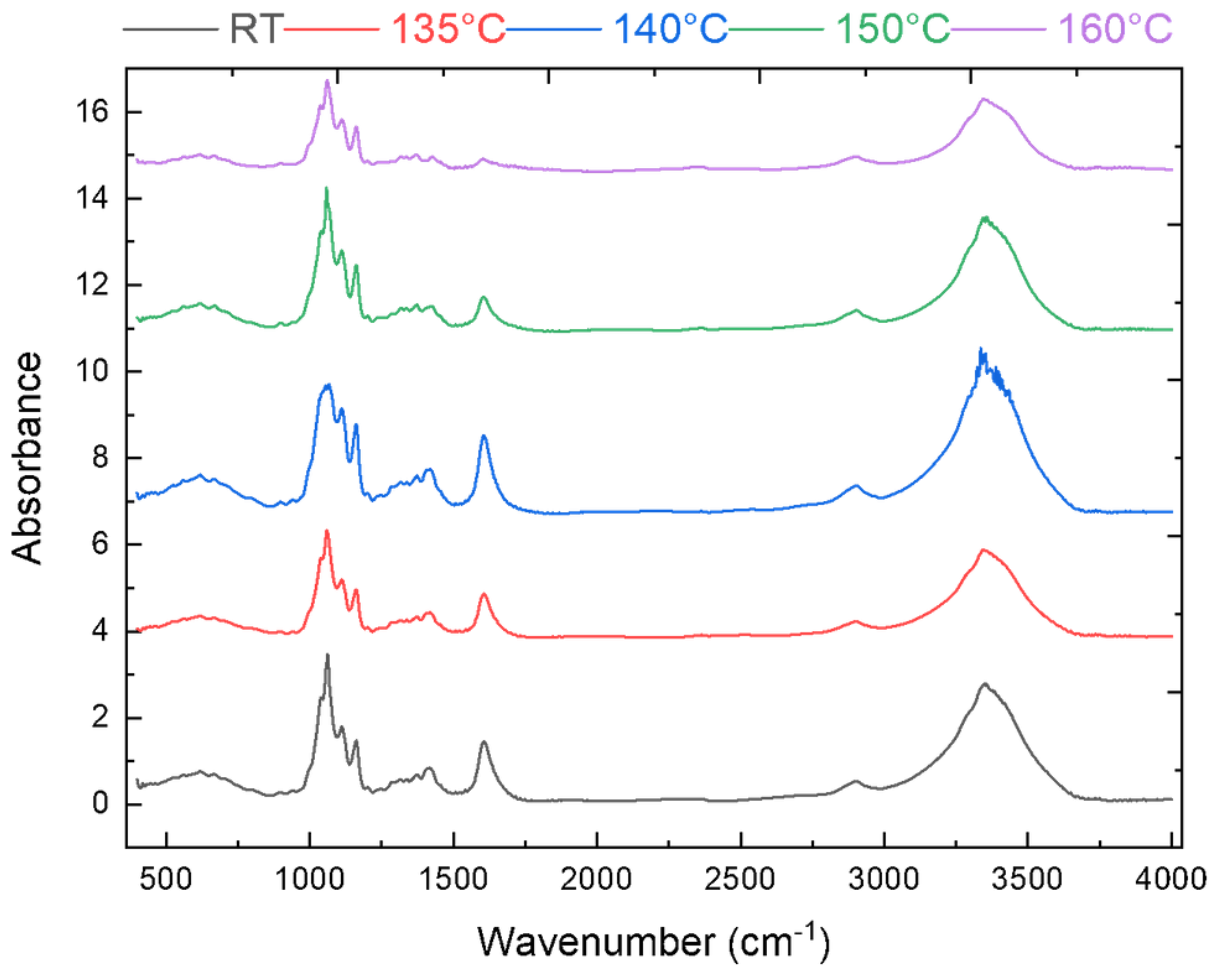

Figure 3

FT-RI spectrum of a 5-μm-thick film sample made by using the as-produced TEMPO-CNFs (a) or the thermally treated TEMPO-CNFs in saturated water vapor at 135°C (b), 140°C (c), 150°C (d), or 160°C (e) for 2 hours. The film samples were measured directly (without folding).

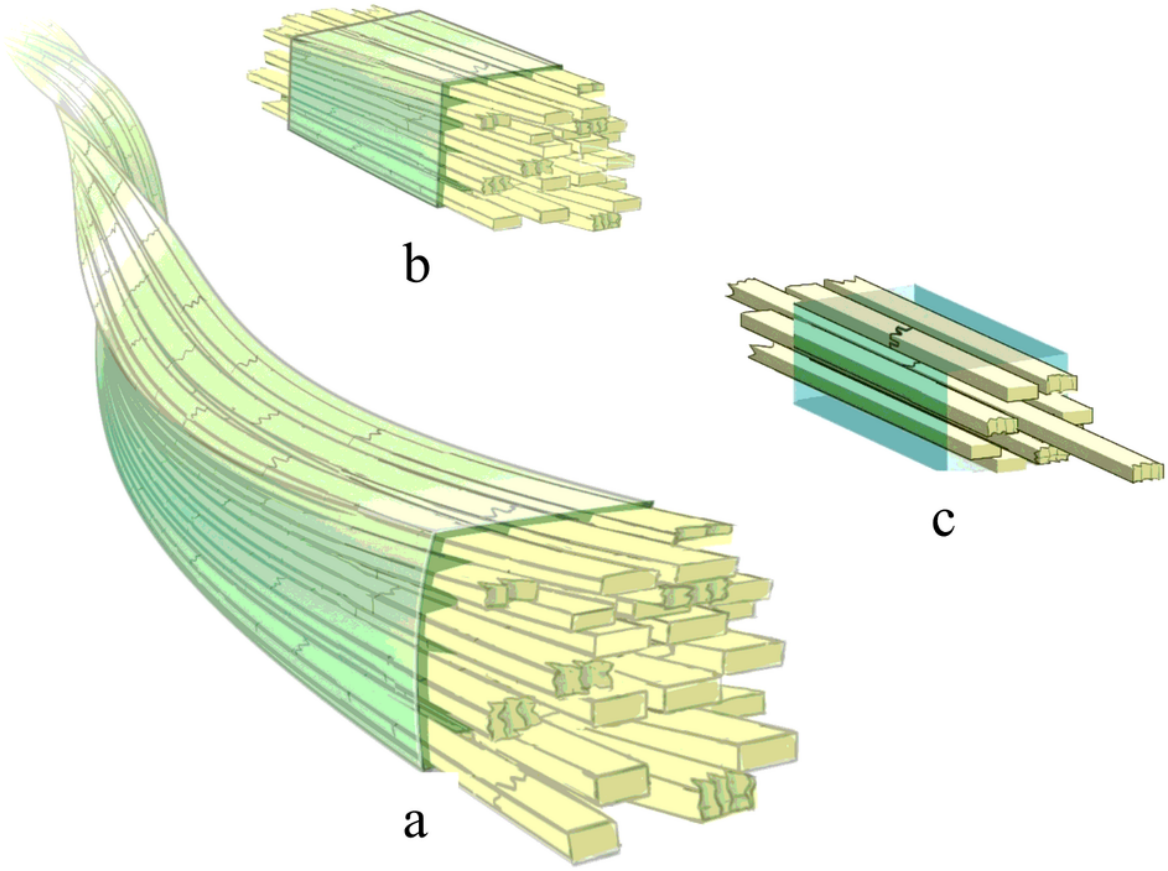

Figure 4

Finger-jointing structures for lengthening cellulose microfibrils. (a) Polysaccharide chains in cellulose microfibrils are not the seamlessly long length of polymers, but relatively short (100s of nm in length), and each of the short chains is jointed in a finger-jointing manner. Finger-jointing is weaker but flexible compared to the packed (vertical) structures. Under tough conditions, such as saturated water vapor at higher temperature/pressure, cellulose microfibrils are unzipped (decomposed) into short blocks starting at the finger-jointing boundaries. (b) Once the microfibril is unzipped into short blocks, (c) polysaccharide chains situated at the outmost layers of the block can be detached from the main body as a thinner block.

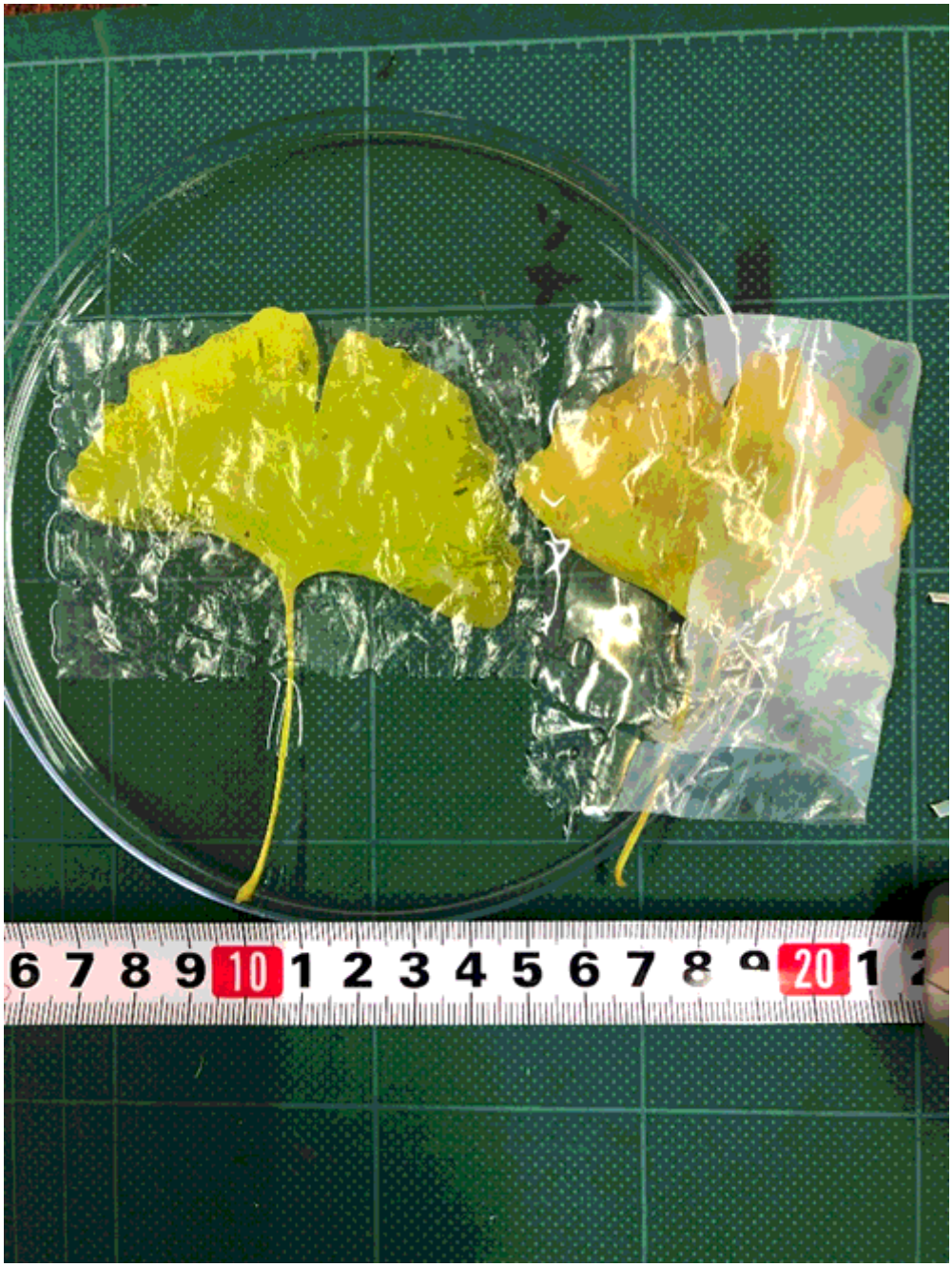

Figure 5

PTFE/CNW (PTFE 99.4%, CNWs 0.6%) hybridized film (thickness 80 □m) is capable of adsorbing water and turning from translucent to transparent. A piece of Ginkgo leaf is placed on the bottom and another Ginkgo leaf is placed half in a polystyrene-based petri dish (□ 15 cm). The dish is filled with water until it is over the leave on the bottom of the dish. A piece of the PTFE/CNW hybridized film is placed over the leaves, absorbing water.